Mineral chemistry of a peralkaline combeite-lamprophyllite nephelinite from Oldoinyo Lengai, Tanzania

J. B. DAWSON AND P. G. HILL

Department of Geology and Geophysics, University of Edinburgh, West Mains Road, Edinburgh EH9 3JW, UK

ABSTRACT

A peralkaline nephelinite lava ([Na+K]/Al 2.15) from the active carbonatite volcano Oldoinyo Lengai, contains combeite, Ba lamprophyllite, a phase with affinities to delhayelite, CeSrNb perovskite, a CaNa phosphate high in Sr, Ba and K, and peralkaline glass; in addition to Fe-rich nepheline, aegirine-rich clinopyroxene and FeK-rich sodalite. The high alkali concentrations relative to alumina in the bulk rock could not have been achieved by fractionational crystallisation of the known Al-rich phenocryst phases (nepheline and sodalite) and some other process must be invoked.

Introduction

THE silicate lavas extruded from the active carbonatite volcano Oldoinyo Lengai, Tanzania (2° 45'S, 35° 54'E), comprise nephelinites, phonolitic nephelinites and phonolites (Dawson, 1962a). The nephelinites associated with the earliest palagonitised pyroclastics that form the bulk of the volcano are olivine-free, and consist of nepheline, clinopyroxene, garnet, apatite, magnetite and glass (Donaldson *et al.*, 1987). However, the nephelinites forming blocks in, interbedded with and post-dating the later black pyroclastic series can contain the additional relatively-unusual phases vishnevite, wollastonite and combeite ($Na_2Ca_2Si_3O_9$).

During an earlier study of Oldoinyo Lengai silicate lavas, Donaldson *et al.* (1987) identified a nephelinite block derived from the black pyroclastics (specimen BD70) as being of particular interest. It is exceptionally peralkaline [(Na + K)/Al 2.15], and the light-microscope examination had identified globular patches within the groundmass containing 'loparite', deep-green glass, and two unidentified phases - one a colourless NaCa silicate, the other an orange-brown KNaBaSrTi silicate. The results presented here arise from an investigation of the two unidentified phases, now known to be combeite

and lamprophyllite respectively, during which other previously unsuspected minerals were found.

Petrography

Petrographic examination was made by a combination of light microscopy and back-scattered electron imaging (BSEI), the latter technique being of particular value in the examination of the fine-grained groundmass and for proving zoning.

The rock is porphyritic, with euhedral phenocrysts (>1 mm) of nepheline (up to 5 mm) (~24 vol.%), sodalite (4.9%), combeite (1%), clinopyroxene (2.6%), titanite (0.3%) and Ti-andradite (0.4%) and rounded grains of apatite (1%). Combeite, titanite and Ti-andradite are phenocryst phases identified additional to those reported by Donaldson *et al.* (1987) and their vishnevite/cancrinite, identified optically, is here identified as sodalite by electron-probe micro-analysis (EPMA). Nepheline and pyroxene contain mutual inclusions, pointing to co-precipitation, and both contain inclusions of garnet. Garnet also occurs as discrete phenocrysts and in aggregates with phenocrystal titanite.

Most phenocryst species are zoned, visible zoning being picked out by variations in inclusion density (in nepheline and combeite; Fig. 1a and b),
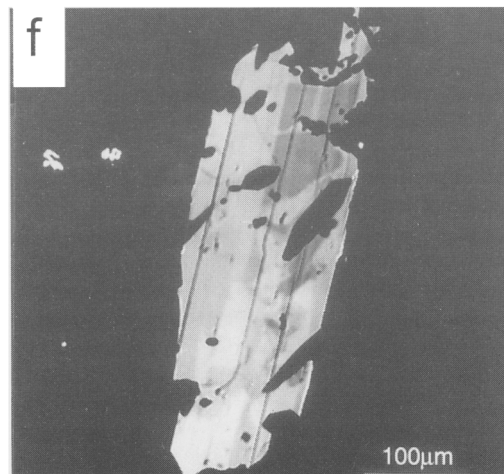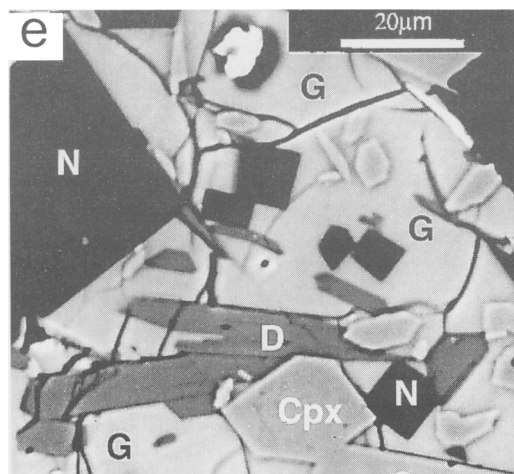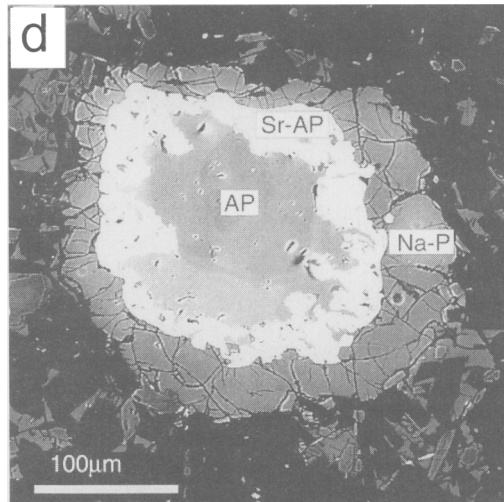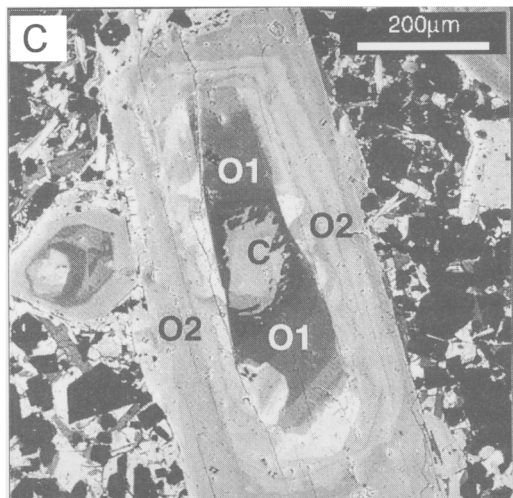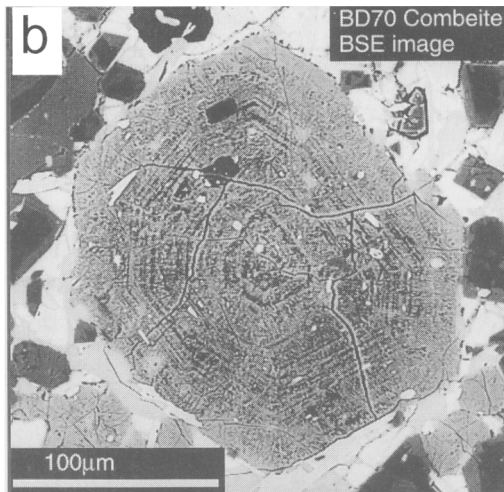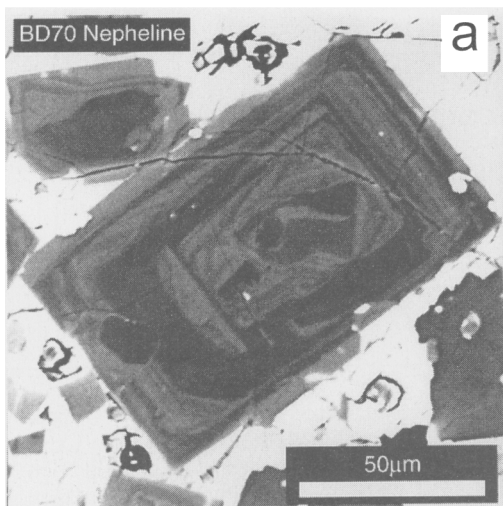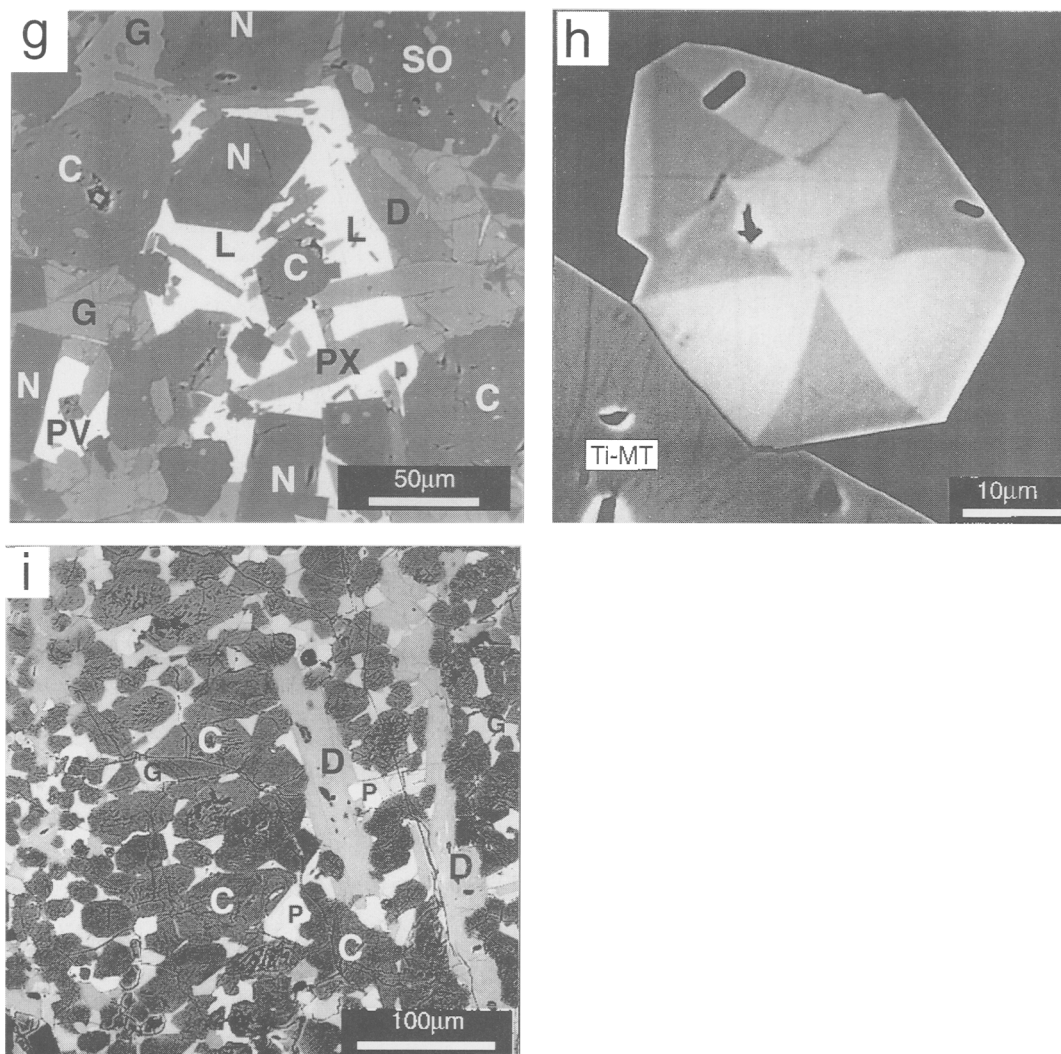
Fig. 1. Back-scattered electron images of phases in BD70. (a) Zoned phenocryst of nepheline (centre of image). Variations are due mainly to differences in Fe. Microphenocrysts (example at top left) are similarly zoned. (b) Combeite phenocryst, showing concentric growth zones and inclusions of garnet and pyroxene (white) and nepheline (dark grey). (c) Clinopyroxene phenocryst, showing corroded core (C), surrounded by a first overgrowth (O1) of pyroxene, surrounded by a second overgrowth (O2). For analyses, see table 4 and, for trends in Overgrowths 1 and 2, Fig. 2. (d) Apatite (AP) replaced by high-Sr apatite (Sr-AP), and mantled by nefedovite (NaP). (e) Acicular phase resembling delhayelite (D) in patch of groundmass glass (G), with euhedral grains of nepheline (N) and clinopyroxene (Cpx). (f) Bladed lamprophyllite showing light and dark areas. The lighter areas contain relatively high concentrations of Ba (Table 9). The inclusions are of clinopyroxene. (g) Oikocrystic lamprophyllite (L) surrounding zoned nepheline (N), combeite (C), 'delhayelite' (D) and clinopyroxene (PX). Other phases present are inclusion-rich sodalite (SO), glass (G) and perovskite (PV). (h) Sector-zoned CeSrNb perovskite. The brighter zones contain more *REE* than the darker (Table 12a). The other phase is titaniferous magnetite (Ti-MT). (i) Globular groundmass patch, comprising microphenocrysts of combeite (C), set in a matrix of glass (G) together with blades of 'delhayelite' (D) and bright grains of perovskite (P).

colour (in pyroxene and Ti-andradite), and birefringence (sodalite). The internal variations in the pyroxenes and nephelines are particularly marked (Fig.1a and c), with rounded, resorbed cores being overgrown by zoned overgrowths. In the pyroxenes, the zoning culminates in inclusion-rich rims that have the same deep-green colour as the rims of groundmass microphenocrysts. BSE imaging of nepheline, combined with EPMA, shows internal variations that are due mainly to differing Fe contents (Fig. 1a). BSE imaging of apatite grains (Fig. 1d) shows two stages of replacement of original apatite: (i) initial replacement of apatite cores by a high-Sr variety of apatite; and (ii) subsequent marginal replacement by aggregates of a birefringent (2nd-order green maximum) Na-rich phosphate that, in some cases, completely replaces the original grain. EPMA has proved optically-undetectable zoning in titanite.

The groundmass consists of microphenocrysts (<1 mm) and glass; microphenocrysts are of equant euhedral nepheline, sodalite and Ti andradite, acicular grains of clinopyroxene and a phase resembling delhayelite (Fig. 1e), rounded grains of combeite, and tiny 10–20 μm equant grains of high-Ce perovskite. Lamprophyllite (the orange-brown phase recognised by Donaldson et al. (1987) occurs both as distinct bladed grains (Fig. 1f) or as oikocrysts surrounding other groundmass phases (Fig. 1g). Like the phenocrysts, the nepheline microphenocryts are strongly zoned and the clinopyroxene grains are zoned from light-green cores to dark-green rims. The perovskite displays good sector twinning in BSEI (Fig. 1h) and, although some garnet grains are homogeneous, others have proved to be slightly zoned. Other groundmass grains are homogeneous, though BSEI of some lamprophyllite grains shows patchy variations (Fig. 1f). Also in the groundmass are rare, tiny (<20 μm) grains of pyrrhotite and magnetite. Globular patches in the groundmass measuring up to 2 × 1 mm were interpreted by Donaldson et al. (1987) as segregation vesicles; they comprise concentrations of combeite, perovskite and glass (Fig. 1i) and, occasionally, 'delhayelite' and oikocrystic lamprophyllite.

Whole-rock chemistry

The whole-rock chemistry (from Donaldson et al., 1987) is given here as a background to the mineral chemistry section below: SiO_2 44.13 wt.%, TiO_2 1.05, Al_2O_3 13.05, Fe_2O_3 5.59, FeO 3.83, MnO 0.38, MgO 0.80, CaO 7.65, Na_2O 13.53, K_2O 5.43, P_2O_5 0.54, SO_3 0.92, H_2O^+ 1.01, CO_2 0.19, sum 98.11 wt.%, (Na+K)/Al = 2.15. Trace elements present in high concentrations (ppm) are Zn 322, Rb 134, Sr 2735, Y 31, Zr 852, Nb 330, Ba 2634, Pb 43, Li 46, Cl 7800, F 2180, U 9, Th 10. Compared with other members of the Oldoinyo Lengai silicate lava suite, BD70 has some of the lowest SiO_2 and Al_2O_3 concentrations; it also has the highest concentrations of total iron, Na_2O, Cl and F, and amongst the highest concentrations of K_2O, Zn, Rb, Zr, Nb, Sr and Ba. It is one of the least oxidised of the lava suite, with a $FeO/(FeO+Fe_2O_3)$ value of 0.41 (suite range is 0.44 to 0.11).

Mineral chemistry

Analytical methods

The minerals were analysed by W.D.S. techniques on a Camebax Microbeam electron microprobe at the University of Edinburgh. Standards used were: for Si and Ca — wollastonite; Ti — rutile; Al — corundum; Fe, Mn, Nb, U and Th — metals; Mg — periclase; Na — jadeite; K — orthoclase; P — apatite; Ba — barite; Sr and S —

TABLE 1. Nephelines in BD70

	1	2	3	4	5
SiO_2	41.3	42.3	42.4	41.5	40.3
Al_2O_3	33.2	31.7	31.3	27.5	28.0
Fe_2O_3	0.90	2.39	2.39	7.34	8.02
CaO	0.26	0.02	0.00	0.02	0.00
Na_2O	15.5	15.2	15.3	15.4	15.2
K_2O	8.12	7.85	7.79	8.19	8.30
Sum	99.28	99.46	99.18	99.95	99.82

Total Fe as Fe_2O_3

Cations per 4 oxygens

	1	2	3	4	5
Si	1.015	1.038	1.043	1.038	1.013
Al	0.962	0.916	0.905	0.809	0.829
Fe^{3+}	0.017	0.044	0.044	0.138	0.152
Ca	0.007	0.001	0.000	0.000	0.000
Na	0.736	0.722	0.733	0.745	0.740
K	0.255	0.246	0.245	0.261	0.266
Sum	2.992	2.967	2.970	2.991	3.000
K/(K+Na)	0.257	0.254	0.250	0.259	0.264

1, 2 Core and rim of phenocryst.
3, 4, 5 Core. intermediate zone and rim of groundmass grain

celestite; the rare earths — synthetic *REE*-bearing CaAl silicate glasses prepared in Edinburgh; Cl — halite; F — MgF_2; Zr — zircon. Spectrometer and analysing crystal configurations were selected to accommodate different mineral chemistries and to obviate peak and background overlaps. In all cases, Na and K were analysed early in the routine to avoid migration/volatility effects. Counting times were 30 seconds on peaks, except for the *REE*, Nb, U and Th when counting on peaks was for 60 seconds; background counts were made for half the peak times. Most minerals were analysed with a spot beam of ~ 1 µm at 20 kV and a probe current of 20 nA (measured by Faraday cup), but combeite, sodalite, 'delhayelite', the CaNa phosphate and the glasses proved to be unstable under these conditions, so were analysed at 10 nA with the beam rastered over a 12.5 µm square. Data were reduced using the correction procedure known as the PAP routine (Pouchou and Pichoir, 1991).

Phenocrysts
Nepheline
Phenocryst cores contain excess Si and around 25% Ks molecule. Although some are homogeneous, others are particularly complex with zones and patches with differing K and Fe concentrations (Fig. 1*a*). Enrichment in K is a general feature of the grain rims (Table 1). The only minor element of note is Fe which, like K, is more highly concentrated in the rims (2.39 wt.% Fe_2O_3 *vs* <1 wt.% in the cores — all Fe calculated as Fe_2O_3). Donaldson *et al.* (1987) found the Ne:Ks ratio of other Oldoinyo Lengai nephelines increases with increasing SiO_2 content of the bulk rocks, with ratios varying from ~ 3 in the least siliceous nephelinites to 5.5 in phonolites; the low Ne:Ks ratio (3) of the nephelines in BD70 is consistent with the whole-rock low SiO_2 content. Overall, the nephelines are slightly more potassic than those in ijolite xenoliths from the volcano (Dawson *et al.*, 1995*a*).

TABLE 2. Representative analyses of combeite in BD70

	1	2	3	4	5	6	7	8	9	10
SiO_2	50.3	50.0	50.1	50.4	49.8	50.2	50.2	50.3	49.9	50.11
TiO_2	0.22	0.06	0.01	0.03	0.18	0.17	0.06	0.11	0.09	0.24
Al_2O_3	0.01	0.01	0.00	0.02	0.00	0.00	0.00	0.00	0.02	0.00
FeO	2.82	2.76	2.95	2.54	2.82	2.61	2.64	2.67	3.03	0.95
MnO	0.89	0.91	0.93	0.85	0.87	0.76	0.78	0.88	0.87	0.68
MgO	0.14	0.15	0.15	0.13	0.14	0.14	0.12	0.14	0.16	0.20
CaO	22.1	21.8	22.4	22.2	22.3	22.6	22.8	22.3	21.5	28.04
Na_2O	22.8	23.2	22.7	22.7	23.0	22.9	22.7	22.7	23.3	20.39
K_2O	0.10	0.08	0.12	0.08	0.08	0.10	0.10	0.10	0.12	0.38
SO_3	0.02	0.00	0.04	0.05	0.04	0.00	0.00	0.04	0.08	n.a.
Sum	99.38	98.87	99.40	98.90	99.23	99.48	99.30	99.24	99.07	100.99
Total Fe as FeO										
Cations per 9 oxygens										
Si	3.000	2.998	2.998	3.015	2.978	2.995	3.001	3.006	2.992	2.967
Ti	0.010	0.003	0.001	0.001	0.008	0.008	0.002	0.005	0.004	0.011
Al	0.001	0.001	0.000	0.002	0.000	0.000	0.000	0.000	0.002	0.000
Fe	0.141	0.138	0.147	0.127	0.141	0.130	0.132	0.134	0.152	0.047
Mg	0.013	0.014	0.014	0.012	0.013	0.013	0.010	0.013	0.014	0.020
Mn	0.045	0.046	0.047	0.043	0.044	0.039	0.040	0.045	0.044	0.034
Ca	1.412	1.402	1.431	1.424	1.428	1.441	1.458	1.431	1.381	1.779
Na	2.635	2.697	2.626	2.631	2.666	2.652	2.626	2.627	2.710	2.339
K	0.008	0.006	0.009	0.006	0.006	0.008	0.008	0.008	0.009	0.028
S	0.001	0.000	0.002	0.002	0.002	0.000	0.000	0.000	0.004	0.000
Sum	7.265	7.305	7.275	7.263	7.286	7.286	7.277	7.269	7.308	7.225
na	0.65	0.66	0.65	0.65	0.65	0.65	0.64	0.65	0.66	0.57

na = Na/(Na + Ca)

1, 2. Core and rim of phenocryst. 3–7. In groundmass globule with loparite and glass. 8, 9. In a different globule. 10. Combeite replacing wollastonite, in lapillus from 1966 eruption, Oldoinyo Lengai (Dawson *et al.*, 1989).

Combeite

Combeite is a Na Ca silicate but, in those from BD70, Fe and Mn are substantial minor elements (Table 2). Despite evidence from micro-inclusions of several stages of concentric growth (Fig. 1*b*), rim compositions are essentially the same as cores. Dawson *et al.* (1989) found that other combeites from Oldoinyo Lengai have excess Na over the simplified $Na_2Ca_2Si_3O_9$ composition, with combeite formed by replacement of wollastonite and clinopyroxene as the result of postulated interaction with natrocarbonatite during the 1966 ash eruption having a

Na/(Na+Ca) ratio of ~ 0.58. The BD70 combeite, which is clearly magmatic, is more sodic with Na/(Na+Ca) ~ 0.66.

Sodalite

Compared with most other sodalites reported in the literature (Deer *et al.*, 1971, Table 36), the sodalite in BD70 (Table 3) is distinctive in two respects. It is considerably higher in Fe_2O_3 (2.68 to 3.52 wt.% *vs* a maximum of 0.85 wt.% reported by Deer *et al.*). It also contains substantial K_2O (3.28 to 4.13 wt.%), with a commensurate reduction in the Na_2O concentrations, compared

TABLE 3. Sodalites in BD70 and, for comparison, from the Kola Penisula

	1	2	3	4	5	6	7
SiO_2	36.6	36.5	36.3	36.6	36.2	35.9	36.69
Al_2O_3	28.9	27.9	27.9	28.0	28.0	28.4	31.40
Fe_2O_3	2.68	3.47	3.52	3.12	3.52	3.27	0.85
MnO	0.04	0.03	0.06	0.05	0.05	0.00	n.a.
MgO	0.12	0.07	0.07	0.09	0.08	0.04	n.a.
CaO	0.19	0.02	0.06	0.05	0.09	0.14	0.19
Na_2O	22.3	22.5	22.9	22.6	22.6	22.6	25.96
K_2O	4.13	3.83	3.28	3.77	3.76	3.64	0.28
P_2O_5	0.13	0.01	0.05	0.03	0.04	0.04	n.a.
SO_3	0.82	0.55	0.43	0.77	0.82	0.46	0.38
Cl	6.57	6.71	6.67	6.41	6.61	6.64	5.64
F	0.00	0.00	0.00	0.17	0.17	0.16	n.a.
Sum	102.44	101.59	101.26	101.66	101.94	101.24	101.71
$O \equiv Cl, F$	1.48	1.51	1.50	1.51	1.57	1.57	1.39
Total	100.96	100.08	99.76	100.15	100.37	99.67	100.32

Structural formulae on basis of 12 Si + Al + Fe^{3+}

	1	2	3	4	5	6	7
Si	6.034	6.063	6.066	6.106	6.046	5.995	5.993
Al	5.632	5.558	5.491	5.501	5.512	5.594	5.986
Fe3+	0.334	0.379	0.443	0.393	0.442	0.411	0.102
Mn	0.006	0.011	0.007	0.006	0.007	0.000	0.000
Mg	0.029	0.023	0.018	0.024	0.021	0.009	0.000
Ca	0.034	0.002	0.011	0.009	0.009	0.025	0.033
Na	7.167	7.148	7.438	7.314	7.326	7.332	8.138
K	0.869	0.845	0.698	0.802	0.801	0.773	0.047
P	0.019	0.002	0.007	0.004	0.006	0.006	0.000
S	0.102	0.093	0.054	0.097	0.103	0.058	0.115
Cl	1.834	1.825	1.887	1.814	1.867	1.879	1.546
F	0.000	0.000	0.000	0.091	0.090	0.087	0.000
Sum	22.060	21.919	22.120	22.161	22.230	21.396	21.960

1, 2, 3. Core, intermediate zone and rim of optically-zoned phenocryst.
4, 5. Core and rim of phenocryst.
6. Groundmass microphenocryst.
7. In nepheline syenite, Kola Peninsula (Fersman and Bonshtedt, 1937); total contains 0.30 wt.% H_2O^+ and 0.04 wt.% H_2O^-.

with concentrations of not more than 0.46 wt.% in most other reported examples. Sodalite from another combeite nephelinite from Oldoinyo Lengai (Peterson, 1989) has the same chemical characteristics as those reported here. In BD70 the phenocrysts are both chemically- and optically-zoned, with the rims containing higher Fe_2O_3 but lower K_2O than the cores (cf. Table 3, analyses 1 and 3).

Clinopyroxene

The clinopyroxene phenocrysts consistently have rounded, resorbed. broadly-zoned cores overgrown by pyroxene characterised by a series of narrower, planar-faced zones. The crystal illustrated in Fig. 1c, and for which analyses are given in Table 4, is more complex than usual in that the corroded core is overgrown by composi-

tionally-different pyroxene that represents *two* further episodes of pyroxene precipitation, themselves separated by a stage of resorbtion.

The bulk of the compositions can be expressed in terms of variations in the molecular proportions of aegirine, diopside and hedenbergite; overall the pyroxene is low in alumina (<1.50 wt.%) and , with the exception of the rim, TiO_2 (<0.80 wt.%). The core (Table 2, analyses 1 and 2) consists of two zones both of which contain ~ 18 wt.% aegirine molecule, but the outer zone is more magnesian than the inner, i.e the reverse of what might be expected from fractional crystallisation. Overgrowth 1 (O1 on Fig. 1c) consists of relatively broad zones (up to 60 μm) which change composition consistently outwards towards more sodic and iron-rich compositions, and the overall trend is also towards greater

TABLE 4. Pyroxene phenocryst in BD70

	1	2	3	4	5	6	7	8	9	10	11	12	13	14
SiO_2	50.3	50.7	52.1	51.7	51.5	51.1	50.9	49.1	50.3	49.5	49.4	49.8	50.5	50.6
TiO_2	0.46	0.41	0.70	0.49	0.44	0.37	0.38	0.56	0.48	0.61	0.79	0.54	0.43	2.16
ZrO_2	0.06	0.04	0.06	0.09	0.01	0.06	0.00	0.06	0.07	0.10	0.00	0.01	0.00	0.08
Al_2O_3	1.02	0.84	0.79	0.79	0.74	0.79	0.83	1.03	0.91	1.10	1.50	1.05	0.62	0.37
Fe_2O_3	6.55	6.50	2.32	3.25	3.77	4.53	4.94	10.4	6.93	8.02	7.10	7.47	6.91	24.1
FeO	11.3	9.83	5.98	6.59	8.09	10.1	9.60	12.2	10.2	10.8	9.43	10.9	10.3	4.47
MnO	0.62	0.53	0.26	0.30	0.39	0.51	0.48	0.69	0.56	0.59	0.51	0.59	0.56	0.27
MgO	6.95	7.88	12.6	11.8	10.6	8.85	8.97	4.40	7.52	6.64	7.73	6.76	7.45	1.91
CaO	20.2	20.4	23.5	23.4	22.7	21.8	21.6	17.9	20.3	19.9	20.9	20.0	20.2	5.47
Na_2O	2.26	2.25	0.88	0.94	1.18	1.55	1.60	3.36	2.25	2.36	1.98	2.34	2.23	10.2
Sum	99.72	99.38	99.16	99.35	99.42	99.70	99.30	99.70	99.52	99.62	99.34	99.46	99.30	99.63

Cations per 6 oxygens
| Si	1.952	1.958	1.961	1.955	1.960	1.963	1.959	1.934	1.948	1.927	1.913	1.939	1.960	1.960
Ti	0.013	0.012	0.020	0.014	0.013	0.011	0.011	0.017	0.014	0.018	0.023	0.016	0.012	0.063
Zr	0.002	0.001	0.001	0.002	0.000	0.001	0.000	0.001	0.001	0.002	0.000	0.000	0.000	0.002
Al	0.047	0.039	0.035	0.035	0.033	0.036	0.038	0.048	0.041	0.050	0.069	0.048	0.027	0.017
Fe^3	0.191	0.190	0.066	0.093	0.108	0.131	0.143	0.307	0.202	0.235	0.207	0.219	0.197	0.701
Fe^{2+}	0.368	0.317	0.188	0.208	0.258	0.324	0.309	0.401	0.331	0.351	0.306	0.356	0.329	0.145
Mn	0.020	0.018	0.008	0.010	0.013	0.017	0.016	0.023	0.018	0.019	0.017	0.020	0.018	0.009
Mg	0.401	0.453	0.708	0.668	0.603	0.506	0.514	0.258	0.434	0.385	0.447	0.392	0.442	0.110
Ca	0.837	0.845	0.949	0.947	0.925	0.897	0.893	0.756	0.841	0.834	0.869	0.833	0.848	0.227
Na	0.170	0.178	0.064	0.069	0.089	0.115	0.119	0.256	0.169	0.178	0.149	0.177	0.168	0.767
Sum	4.001	4.011	4.000	4.001	4.002	4.001	4.002	4.001	3.999	3.999	4.000	4.000	4.001	4.001
$\frac{Fe^{2+}}{(Fe^{2+}+Fe^{3+})}$	0.66	0.63	0.73	0.70	0.67	0.71	0.68	0.56	0.62	0.59	0.59	0.62	0.62	0.17

1, 2 Centre and edge of corroded core; 3−7 successive optically distinctive zones in overgrowth 1; 8−14 are successive optically distinctive oscillatory zones in overgrowth 2; analysis 14 rim crowded with numerous small inclusions of Ti-andradite and Ti magnetite, and compositionally similar to Na Fe-rich groundmass pyroxenes (Table 8).

oxidation of the iron (Fig. 2). Compared with the core, the compositions in Overgrowth 1 are considerably more magnesian, the iron is not as oxidised, and they contain lower concentrations of TiO_2 and Al_2O_3. Overgrowth 2 (O2 on Fig. 1c) consists of finer (15−20 μm) zones of pyroxene that, in general, is more sodic and iron-rich than in Overgrowth 1 but rather similar to the core pyroxene. Moreover, the zoning is oscillatory, but the compositional variations are not consistent with fractional crystallisation; apart from the extreme rim, the earliest zone is the most sodic and iron-rich (analysis 8) whereas later zones are more diopsidic. There is repetition of some compositions (e.g. analyses 9 and 13, and 10 and 12) but there is no set pattern. The extreme rim (Table 4, analysis 14) is crowded with numerous small inclusions of Ti andradite and magnetite; it is very sodic (10.2 wt.% Na_2O) and contains very high amounts of (calculated) ferric iron (24.1 wt.% Fe_2O_3)), and also the highest amounts of TiO_2 (2.16 wt.%). There is a major compositional gap between the rim and the other zones in Overgrowth 2.

The corroded core/zoned overgrowth relation-ship, and reversion of some zones to more magnesian compositions, are features common to the pyroxene phenocrysts in many other lavas from Oldoinyo Lengai, and also in the pyroxenes in plutonic ijolites and pyroxenite xenoliths from the volcano. In the latter, this has been attributed to a combination of magma chamber convection and new injections of magma (Dawson et al., 1995a).

Ti-andradite

The garnet (Table 5) falls within the composi-tional range of garnet reported in other lavas and ijolites from Oldoinyo Lengai (Donaldson et al., 1987; Dawson et al., 1995a). The main composi-tional variations are in the amounts of Ti and total Fe, which vary inversely. The Fe tends to be less oxidised in the higher-Ti grains and zones, which are also the most magnesian. Of the minor elements, Na_2O (0.57 wt.%), MnO (0.42%) and ZrO_2 (0.72%) are present in appreciable amounts (values are maximun concentrations). In the analysed grains, there is no consistent sense of
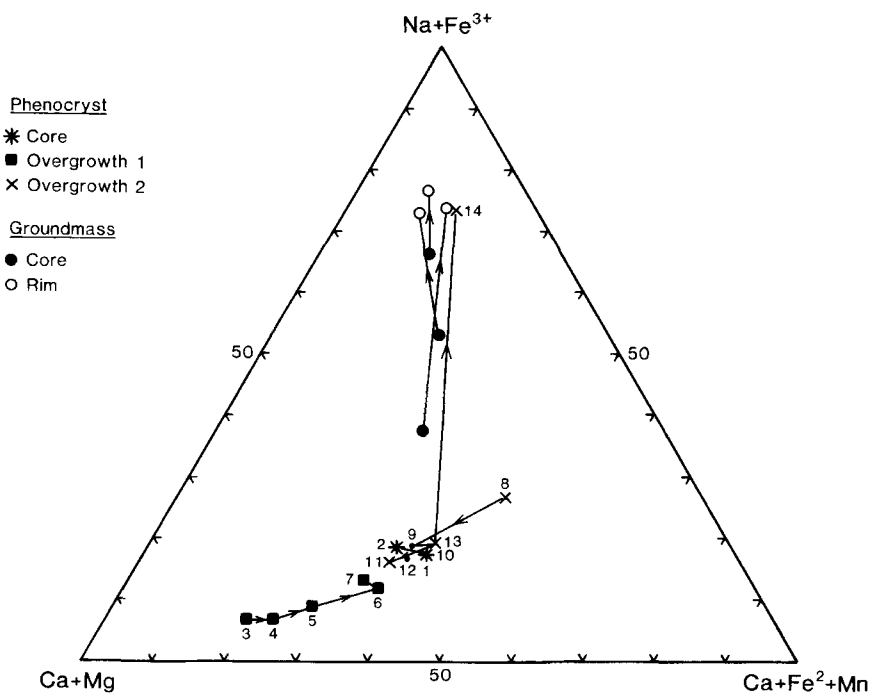
Fig. 2. Aegirine-diopside-hedenbergite plot for pyroxene phenocryst and groundmass microphenocrysts. Data from Tables 4 and 8; numbers for phenocryst points refer to analyses in Table 4.

TABLE 5. Garnets in BD70

	1	2	3	4	5	6	7	8	9	10
Nb_2O_5	0.00	0.01	0.70	0.00	0.09	0.01	0.05	0.04	0.00	0.02
SiO_2	30.8	31.4	31.2	27.2	26.8	29.1	29.6	28.9	29.7	31.1
TiO_2	9.59	8.29	9.10	16.4	16.3	12.8	12.6	13.2	11.4	10.8
ZrO_2	0.18	0.27	0.26	0.64	0.72	0.53	0.42	0.44	0.67	0.50
Al_2O_3	0.67	0.70	0.86	0.50	0.60	0.98	0.58	1.00	0.63	0.58
Ce_2O_3	0.00	0.02	0.09	0.15	0.08	0.08	0.03	0.06	0.07	0.04
Fe_2O_3	20.5	21.8	20.9	13.8	13.8	16.8	17.7	16.4	18.6	19.5
FeO	4.46	3.59	3.76	7.37	7.68	5.91	5.61	6.18	5.50	4.90
MnO	0.35	0.36	0.35	0.34	0.34	0.37	0.42	0.38	0.43	0.46
MgO	0.26	0.25	0.34	0.84	0.96	0.63	0.40	0.59	0.39	0.36
CaO	31.8	32.1	32.2	31.7	31.6	31.7	31.6	31.9	31.3	30.7
SrO	0.00	0.02	0.01	0.00	0.00	0.05	0.10	0.00	0.02	0.05
Na_2O	0.43	0.35	0.31	0.43	0.42	0.33	0.57	0.33	0.40	0.57
Sum	99.04	99.16	100.08	99.37	99.39	99.27	99.68	99.42	99.11	99.58
FeO^T	22.87	22.35	22.53	19.83	19.81	21.04	21.53	20.93	22.25	22.40
Cations per 24 oxygens										
Nb	0.000	0.001	0.051	0.000	0.007	0.001	0.004	0.003	0.000	0.002
Si	5.306	5.345	5.309	4.718	4.676	5.018	5.076	4.974	5.134	5.308
Ti	1.241	1.070	1.165	2.141	2.129	1.657	1.632	1.713	1.480	1.389
Zr	0.015	0.023	0.021	0.054	0.061	0.004	0.035	0.037	0.056	0.042
Al	0.139	0.142	0.173	0.101	0.123	0.199	0.117	0.203	0.128	0.117
Fe^{3+}	2.649	2.640	2.674	1.808	1.804	2.179	2.287	2.124	2.322	2.503
Ce	0.000	0.001	0.000	0.009	0.005	0.005	0.002	0.004	0.005	0.002
Fe^{2+}	0.642	0.576	0.535	1.069	1.083	0.851	0.805	0.891	0.794	0.701
Mn	0.051	0.052	0.051	0.050	0.050	0.054	0.060	0.056	0.063	0.067
Mg	0.067	0.063	0.087	0.212	0.250	0.161	0.103	0.152	0.100	0.088
Ca	5.859	5.855	5.870	5.892	5.896	5.855	5.820	5.892	5.800	5.626
Sr	0.000	0.002	0.001	0.000	0.000	0.005	0.010	0.000	0.002	0.005
Na	0.145	0.117	0.102	0.114	0.141	0.111	0.189	0.111	0.134	0.188
Sum	16.114	15.886	16.039	16.168	16.225	16.100	16.136	16.157	16.018	16.038
fe	0.196	0.179	0.167	0.371	0.375	0.280	0.260	0.296	0.246	0.218

$fe = Fe^{2+}/(Fe^{2+} + Fe^{3+})$
1, 2 Core and rim of grain included in nepheline phenocryst.
3−6 Inclusions in zoned pyroxene phenocryst: 3, 4 core and rim of grain at pyroxene core/mantle boundary;
5 homogeneous grain in zone midway between pyroxene core and rim;
6 homogeneous grain in pyroxene margin.
7, 8 Homogeneous groundmass grains.
9, 10 Core and rim of slightly-zoned groundmass grain.

zoning, with rims higher in Ti than cores in some grains, whereas the reverse is true in other grains.

Titanite

In addition to Ca, Ti and Si, the titanite contains appreciable Nb_2O_5 (0.83 wt.%), ZrO_2 (0.62%), FeO (2.02%), SrO (0.61%) and, in some, Na_2O (0.59%) (maximum concentrations, Table 6); of the *REE*, only Ce is present in measurable concentrations (up to 0.17 wt.%

Ce_2O_3). There are appreciable variations in the concentrations of these minor oxides between individual homogeneous grains (e.g. SrO 0.12 to 0.61 wt.%; Na_2O 0.08 to 0.59 wt.%), but the inter-grain ranges cover the variations found within the one grain found to be compositionally zoned (Table 6, analyses 3 and 4). In this zoned grain, the rim contains higher Nb, Sr and Na, but lower Zr, Fe and Al, than the core. Compared with titanites in ijolite and nepheline syenites blocks

TABLE 6. Titanites in BD70

	1	2	3	4	5
Nb_2O_5	0.62	0.83	0.24	0.37	0.21
SiO_2	29.8	29.8	29.8	29.9	29.6
TiO_2	37.2	38.6	37.2	38.6	37.5
ZrO_2	0.34	0.08	0.47	0.02	0.62
Al_2O_3	0.34	0.04	0.37	0.06	0.99
Ce_2O_3	0.17	0.05	0.11	0.05	0.03
FeO	2.02	1.32	1.77	1.22	1.70
MnO	0.03	0.01	0.04	0.05	0.03
MgO	0.01	0.02	0.05	0.00	0.03
CaO	28.3	27.1	28.4	27.3	28.3
SrO	0.19	0.61	0.11	0.51	0.12
Na_2O	0.08	0.59	0.13	0.52	0.08
Sum	99.10	99.05	99.44	98.55	99.25

Total Fe as FeO

Cations per 5 oxygens
Nb	0.009	0.013	0.004	0.006	0.003
Si	0.996	0.996	1.003	0.995	0.997
Ti	0.936	0.968	0.937	0.978	0.923
Zr	0.006	0.001	0.007	0.000	0.010
Al	0.015	0.001	0.014	0.002	0.039
Ce	0.002	0.001	0.001	0.000	0.001
Fe	0.057	0.037	0.047	0.034	0.048
Mn	0.001	0.001	0.001	0.001	0.001
Mg	0.000	0.000	0.001	0.001	0.001
Ca	1.013	0.967	1.018	0.975	1.017
Sr	0.004	0.012	0.002	0.010	0.002
Na	0.009	0.038	0.008	0.033	0.005
Sum	3.048	3.035	3.044	3.035	3.047

1,2 Large homogeneous grains.
3, 4 Core and rim of large zoned grain.
5. Small grain included in nepheline phenocryst.

from Oldoinyo Lengai (Dawson *et al.,* 1995*a*), those in BD70 contain less Nb, Zr and *REE*, but higher Sr and Na.

Apatite

The cores of the apatite phenocrysts contain only small amounts of elements other than Ca, P and F (Table 7). SrO (1.43 wt.%) is the only minor oxide of note, and of the *REE* only Ce and La are present in analysable concentrations. SiO_2, the total *REE* oxides and Na_2O concentrations together comprise <1.5 wt.%, so coupled substitutions, such as Ca $\leftrightharpoons$ 0.5 Na + *REE* or Ca + P $\leftrightharpoons$ 0.5 *REE* + Si, which are common in carbonatite apatites (Hogarth, 1989) are very limited. In these respects, the apatite cores resemble apatites in

jacupirangites and ijolites from Oldoinyo Lengai (Dawson *et al.,* 1995*a*).

The core apatite is partly replaced by high-Sr apatite of distinctive composition (Fig.1d). In addition to 10.1 wt.% SrO, it contains ~0.4 wt.% of both Ce_2O_3 and La_2O_3, 3.62 wt.% F (all ~×1.5 the concentrations in the replaced apatite); and 0.14 wt.% Nd_2O_3 and 0.23 wt.% BaO, both of which are below analysable levels in the core apatite. It is apparent that the original apatite reacted with a fluid containing enhanced concentrations of Sr, Ba, the *LREE* and F.

The apatite/Sr apatite grains are themselves surrounded by rims of a CaNa phosphate which may completely replace some apatite grains. Repeat analyses were similar at different points in the same reaction rim and in reactions rims around different grains. In addition to CaO and Na_2O (the latter comprising 21.8 wt.%), it contains appreciable BaO (3.40 %) and K_2O (2.09%). Compared with the Sr apatite, which it is mainly replacing, it contains less *LREE*, Sr and F. It has a low analytical total which may be due to unanalysed oxides, in this paragenesis the most likely being CO_2. Of the high-Na phosphates reported in the literature it is compositionally closest to nefedovite ($Na_5Ca_4[PO_4]_2F$), a phosphate reported to pseudomorph apatite in hyperalkaline pegmatites in the Khibina massif, Kola peninsula, Russia (Khomyakov, 1995). Note, however, that nefedovite (Table 7, anal. 4) is a pure CaNa phosphate, with higher concentrations of these elements than in the BD70 CaNa phosphate. Without X-ray conformation, it would be premature to identify the phase as a SrBaK analogue of nefedovite, though it is worthy of note that high-temperature solid solution substitution of Sr and Ba for Ca and K for Na is common in other minerals from Oldoinyo Lengai (Dawson *et al.,* 1995*b*).

Groundmass phases
Nepheline

The composition of the cores of groundmass nephelines is broadly similar to phenocryst rims (Table 1). However, the rims of groundmass grains are exceptionally rich in Fe (>8 wt.% expressed as Fe_2O_3) and, moreover, are more potassic than the cores - the reverse of what is found in the phenocrysts.

Combeite

Small combeite grains in the groundmass, mainly from the globular segregations, are

TABLE 7. Analyses and structural formulae of phosphates in BD70

	1	2	3	4		1	2	3
P_2O_5	40.8	40.6	36.3	42.1	P	6.100	6.241	6.115
SiO_2	0.75	0.30	0.15	n.a.	Si	0.133	0.054	0.060
Ce_2O_3	0.25	0.41	0.18	n.a.	Ce	0.016	0.028	0.013
La_2O_3	0.26	0.44	0.12	n.a.	La	0.017	0.030	0.009
Nd_2O_3	0.00	0.14	0.00	n.a.	Nd	0.000	0.008	0.000
FeO	0.06	0.11	0.56	n.a.	Fe	0.009	0.019	0.092
MnO	0.03	0.00	0.15	n.a.	Mn	0.003	0.001	0.025
CaO	54.0	46.1	23.2	33.7	Ca	10.245	9.045	4.960
SrO	1.43	10.1	6.48	n.a.	Sr	0.147	1.072	0.749
BaO	0.00	0.23	3.40	n.a.	Ba	0.000	0.018	0.265
Na_2O	0.15	0.16	21.8	22.7	Na	0.052	0.056	8.406
K_2O	0.00	0.06	2.09	n.a.	K	0.000	0.014	0.529
F	2.42	3.62	0.29	2.5	F	1.351	2.096	0.178
Sum	100.15	102.09	94.72	101.8		18.073	18.682	21.401
$-O \equiv F$	1.01	1.52	0.12	1.0				
Total	99.14	100.57	94.60	100.8				

Structural formulae on basis of 26 (O, OH, F)

n.a. - not analysed
1. Corroded apatite core. For textures see Fig. 1d
2. Sr-rich apatite replacing corroded apatite
3. Na-rich overgrowth on apatite/Sr apatite grain
4. Nefedovite, Kuniok, Khibina massif, Kola peninsula (Khomyakov, 1995)

compositionally very similar to combeite phenocrysts (Table 2); there are some small intergrain variations in FeO and MnO.

Sodalite

The groundmass sodalite has the same distinctively-high Fe and K concentrations as the phenocryst sodalite (Table 3), and is most similar to that forming the rims of phenocrysts.

Pyroxene

The acicular groundmass pyroxene grains are strongly zoned. The cores are considerably more sodic than those in the phenocryst pyroxene (save for the extreme rim) with between 37 and 65 mol. % aegirine (Table 8), and also contain more TiO_2. The rims of the groundmass grains are all very sodic, with up to 76 mol.% aegirine molecule, and closely resemble the rim on the pyroxene phenocryst (Table 4, anal. 11); the rims also contain appreciable TiO_2 (up to 2.48 wt.%), again similar to the phenocryst rim. The strong similarity between rim compositions of both phenocrysts and groundmass microphenocrysts,

together with the big compositional gap between the phenocryst rim and other phenocryst zones, give grounds for interpreting the phenocryst rim as an epitaxial overgrowth of later groundmass pyroxene.

Lamprophyllite

Lamprophyllite is a mica-like NaKBaSr titano-silicate. The most variable components are the SrO and BaO concentrations, that vary inversely. Compared with data from the literature (Table 9), the Oldoinyo Lengai lamprophyllites, with BaO up to 19.0 wt.%, are most comparable to barytolamprophyllite from the Gardiner complex, Greenland (Johnsen et al., 1994). They have commensurate low SrO compared with lamprophyllites from other localities. Further, the Oldoinyo Lengai lamprophyllites are less sodic but more potassic than others, and also tend to have lower concentration of MnO.

The bladed Oldoinyo Lengai lamprophyllite grains are not homogeneous, the areas that are brighter in BSE images containing higher BaO, but lower SrO and FeO, than the darker areas. The

TABLE 8. Groundmass clinopyroxenes in BD70

	1	2	3	4	5	6
SiO_2	50.8	50.8	51.5	52.3	50.8	49.8
TiO_2	0.98	1.00	1.59	1.73	0.81	2.08
ZrO_2	0.33	0.14	0.00	0.00	0.07	0.09
Al_2O_3	0.40	0.33	0.33	0.35	0.26	0.30
Fe_2O_3	12.3	24.2	21.8	25.3	17.9	24.2
FeO	10.6	2.97	5.17	3.78	7.24	4.19
MnO	0.60	0.32	0.28	0.26	0.45	0.42
MgO	4.29	2.50	2.64	1.68	3.64	1.79
CaO	14.0	8.02	7.09	5.25	10.8	6.67
Na_2O	5.40	9.43	9.45	10.8	7.19	9.73
Sum	99.43	99.61	99.85	100.05	99.09	99.18
Cations per 6 oxygens						
Si	1.979	1.963	1.983	1.981	1.978	1.944
Ti	0.029	0.029	0.046	0.046	0.024	0.061
Zr	0.006	0.003	0.000	0.000	0.001	0.002
Al	0.018	0.015	0.015	0.015	0.012	0.014
Fe^{3-}	0.380	0.703	0.632	0.722	0.526	0.709
Fe^{2+}	0.327	0.096	0.167	0.120	0.236	0.137
Mn	0.020	0.011	0.009	0.008	0.015	0.014
Mg	0.249	0.144	0.151	0.095	0.212	0.104
Ca	0.583	0.332	0.292	0.213	0.452	0.279
Na	0.408	0.706	0.705	0.797	0.544	0.737
Sum	3.999	4.002	4.000	3.997	4.000	4.011
Aegirine	37.4	73.7	65.8	76.4	53.2	73.5
Diopside	29.4	15.1	15.9	10.1	21.4	10.8
Hedenbergite	33.2	11.2	18.1	13.5	25.4	15.7
$Fe^{2+}/(Fe^{2+}+Fe^{3+})$	0.49	0.12	0.22	0.14	0.31	0.16

1, 2 Core and rim of groundmass pyroxene in patch with loparite and glass
3, 4 Core and rim of pyroxene in cluster with garnet in glass
5, 6 Core and rim of grain in glass patch

composition of oikocrystic lamprophyllite (Table 9, analysis 5) lies within the range found for the bladed grains. Because of the current lack of concensus as to the structure of lamprophyllite, no structural formulae are given in Table 9.

'Delhayelite'

A colourless acicular phase in the groundmass of BD70 is a halogen-rich KCaNa alumino-silicate (Table 10). The very few minerals having these compositional characteristics include carletonite and delhayelite. Carletonite, from Mount St.Hilaire, Quebec (Chao, 1971) contains less alumina and halogens than the BD70 phase, and also different K:Na:Ca ratios. Delhayelite, a phase occurring in combeite-

bearing melilite-nephelinite from Mt.Shaheru, Zaire (Sahama and Hytönen,1957), is compositionally broadly similar (Table 10, analysis 5) but differs in several respects, particularly in the silica, potash, sulphur and water contents. However, Sahama and Hytönen (1957) recognised that, due to admixture with nepheline and alteration products, their analysis was probably only an approximation to the true composition. Compositionally the closest analogy, although the Oldoinyo Lengai mineral contains less SiO_2, is with a phase stated to be delhayelite from the Khibina alkaline massif, Kola Peninsula (Table 10, analysis 4) but which, like the Oldoinyo Lengai mineral, also shows important differences from the Mt.Shaheru delhayelite

TABLE 9. Lamprophyllite analyses

	1	2	3	4	5	6	7	8	9	10	11
SiO_2	29.1	28.9	29.0	28.6	29.5	30.40	30.95	31.50	29.90	29.49	30.92
TiO_2	28.8	27.8	28.5	27.9	28.7	27.48	28.15	30.33	28.68	29.29	31.73
Al_2O_3	0.17	0.18	0.16	0.18	0.18	0.00	0.22	0.12	0.04	0.01	0.31
FeO	3.19	2.96	3.16	2.78	3.11	1.97	4.15	1.97	1.27	2.81	3.77
MnO	0.53	0.50	0.54	0.48	0.53	2.33	1.05	1.41	1.60	1.57	2.01
MgO	0.41	0.40	0.35	0.31	0.42	0.25	0.86	1.08	1.03	0.50	0.31
CaO	1.90	1.74	1.86	1.74	1.83	1.41	1.64	0.53	0.26	0.84	1.68
SrO	6.54	4.88	5.88	4.81	5.92	14.58	7.99	14.46	3.48	20.69	14.66
BaO	15.6	18.5	16.1	19.0	17.4	1.25	10.51	4.93	20.06	0.66	1.12
Na_2O	9.20	9.20	9.32	9.28	8.33	12.35	9.80	11.63	11.99	10.60	10.64
K_2O	2.30	2.56	2.56	2.39	2.40	2.31	1.82	0.60	0.94	0.67	0.99
F	1.64	1.48	1.84	1.89	1.50	1.82	1.45	n.a	n.a	n.a	n.a
Sum	99.38	99.10	99.27	99.26	99.82	100.62	100.83	98.47	99.15	97.16	100.07
Less $O \equiv F$	0.69	0.62	0.77	0.79	0.63	0.77	0.62				
Total	98.69	98.48	98.50	98.47	99.19	99.85	100.21	98.47	99.15	97.16	100.07

Cations per 17 oxygens

Si	3.868	3.672	3.847	3.851	3.931
Ti	2.877	2.657	2.883	2.867	2.847
Al	0.027	0.027	0.026	0.178	0.029
Fe	0.355	0.314	0.356	0.317	0.347
Mn	0.060	0.054	0.062	0.055	0.059
Mg	0.081	0.076	0.069	0.064	0.084
Ca	0.271	0.237	0.268	0.254	0.262
Sr	0.505	0.357	0.459	0.380	0.458
Ba	0.814	0.921	0.850	1.015	0.910
Na	2.376	2.265	2.432	2.455	2.156
K	0.391	0.415	0.444	0.415	0.408
F	0.690	0.596	0.785	0.815	0.632
Sum	11.625	11.591	11.696	11.451	11.491

1−5 In BD70, Oldoinyo Lengai. 1, 2. Dark and bright (in BSE) areas in bladed grain; 3,4. dark and bright areas of another bladed grain. 5. Oikocrystic groundmass grain. In analyses of BD70 grains, total Fe is expressed as FeO; Nb, Zr, Y, Ce and Rb were sought but not found
6. Lamprophyllite, Kukisvumchorr, Khibin, Kola (Vlasov, 1964); total includes 3.87 wt.% Fe_2O_3 and 0.60 wt.% loss on ignition
7. Barian lamprophyllite, Rasvumchorr, Khibin, Kola (Vlasov, 1964); total includes 1.83 wt.% Fe_2O_3, 0.99% H_2O^+ and 0.32% H_2O^-
8, 9. Lamprophyllite and barytolamprophyllite, ijolite pegmatites, Gardiner complex, E Greenland (Johnsen et al., 1994)
10. In fenite, Sarimbi carbonatite complex, Brazil (Haggerty and Mariano, 1983)
11. In nepheline syenite pegmatite, Bearpaw Mountains, Montana, U.S.A (Pecora, 1942)

(Stoppa et al., 1997). Another delhayelite-like phase occurs in a melilitolite from San Venanzo, Italy (Stoppa et al., 1997), but this phase (Table 10, analysis 3) differs from both the Oldoinyo Lengai and Khibina material in containing higher alumina, higher K_2O relative to both CaO and Na_2O, and higher Cl relative to F. Sahama and Hytönen (1959) drew some comparisons between delhayelite and rhodesite (Gard and Taylor, 1957) , but the Oldoinyo Lengai, Khibin and Italian delhayelites differ from rhodesite by being both anhydrous and more aluminous. In view of the uncertainty about the structure of delhayelite (see discussion in Stoppa et al., 1997), no structural formula is given in Table 10.

TABLE 10. Analyses of 'delhayelites'

	1	2			3	4	5
SiO_2	44.6	44.2	→	45.1	47.8	43.1	52.60
TiO_2	0.11	0.06	→	0.29	0.00	0.04	0.09
Al_2O_3	6.18	5.99	→	6.32	6.22	11.5	9.22
FeO	1.65	1.48	→	1.87	0.12	1.85	2.72*
MnO	0.09	0.03	→	0.14	0.05	0.04	0.07
MgO	0.09	0.07	→	0.19	0.03	0.45	1.03
CaO	14.7	14.4	→	14.9	13.6	10.9	7.99
Na_2O	6.94	6.34	→	7.85	6.79	3.52	3.20
K_2O	18.0	17.4	→	18.5	19.5	22.4	9.27
P_2O_5	0.20	0.17	→	0.27	n.a	n.a	n.a
SO_3	0.13	0.08	→	0.24	0.07	0.01	1.31
Cl	3.87	3.79	→	3.95	3.57	4.91	3.91
F	4.09	3.91	→	4.54	4.46	3.38	0.33
Sum	100.45				102.38	102.18	101.02
$-O \equiv Cl, F$	2.69				2.68	2.53	1.01
Total	97.76				99.70	99.65	100.01

1 and 2. Mean and range of 9 analyses of acicular white phase in groundmass of BD70
3. Mean of 3 analyses of delhayelite, Khibin, Russia (Stoppa *et al.*, 1997, *in press*)
4. Mean of 3 analyses of "delhayelite" in melilitolite, San Venanzo, Italy (Stoppa *et al*, 1997, *in press*). Total contains 0.07 wt.% BaO and 0.07 wt.% SrO
5. Delhayelite, in kalsilite melilite-nephelinite, Mt. Shaheru, Zaire (Sahama and Hytönen, 1959). Total includes 5.93 wt.% H_2O^+ and 3.35 wt.% H_2O-. *Iron is Fe_2O_3

Glass

The glasses, which are deep green in colour are, in general, silica-undersaturated and extremely rich in iron (up to 18.5 wt.% FeO) and the alkalies (up to 24.5 wt.% $Na_2O + K_2O$); they are also sodic (Na/[Na+K] 0.67 to 0.76) and hyperalkaline ([Na+K]/Al 8 to 15) and contain appreciable concentrations of SO_3 and halogens (Table 11). Low totals suggest the presence of unanalysed volatiles. In addition to these general chemical characteristics, the three petrographically-different types of glass analysed in this study have certain individual chemical characteristics. That included in nepheline is the least aluminous, resulting in the most peralkaline variety ([Na+K]/Al 15.75). Glass within the ordinary groundmass (Table 11, anal. 2–4) is less peralkaline ([Na+K]/Al 12.7 to 13.2), due to slightly higher alumina concentrations rather than to alkali decrease, and is of reasonably uniform composition. Glass occurring with combeite and perovskite in the groundmass globules, although uniform in other respects, does show some Na_2O variations, resulting in variable (Na+K)/Al values of 8 to 11.9.

For comparison, the glass in a wollastonite nephelinite from Oldoinyo Lengai (Donaldson *et al.*, 1987), although containing up to 16 wt.% $Na_2O + K_2O$, is more siliceous (up to 53.92 wt.% SiO_2) and aluminous, and green and brown glasses in other combeite and wollastonite nephelinites from Oldoinyo Lengai (Peterson, 1989) although containing up to 24 wt.% $Na_2O + K_2O$ (Table 11, analyses 8and 9), are more aluminous, resulting in maximum (Na+K)/Al values of 7.27; they also contain less FeO (10.9 to 16.5 wt.%).

CeSrNb perovskite

Tiny, bright-orange grains in the groundmass were identified as loparite by Donaldson *et al.* (1987). Representative analyses of the phase, that has proved to be sector-zoned (Fig. 1*h*), are given in Table 12*a*. It contains substantial concentra-

TABLE 11. Compositions of glasses in BD70, and other combeite-and wollastonite-nephelinites

	1	2	3	4	5	6	7	8	9
SiO_2	35.5	41.8	42.0	42.0	39.2	41.1	39.6	45.22	47.59
TiO_2	3.05	2.97	3.02	3.24	3.63	3.54	3.51	2.08	2.27
Al_2O_3	2.27	2.85	2.79	2.73	3.00	3.22	3.22	4.64	4.54
FeO	17.1	17.4	17.5	17.7	17.4	18.4	18.5	14.80	16.46
MnO	0.82	0.86	0.83	0.80	0.61	0.76	0.67	0.65	0.73
MgO	0.38	0.39	0.38	0.42	0.39	0.49	0.44	0.60	0.65
CaO	1.28	0.15	1.26	1.16	1.30	1.45	1.34	2.78	2.02
Na_2O	16.7	16.7	16.7	17.0	16.6	10.8	12.9	15.07	13.92
K_2O	7.85	7.99	7.88	7.58	7.73	7.42	7.36	8.27	8.39
P_2O_5	0.58	0.88	0.95	0.87	0.70	0.61	0.56	0.50	n.a.
SO_3	3.26	3.62	3.84	3.55	3.91	3.24	4.55	n.a.	n.a.
Cl	0.49	0.35	0.41	0.29	0.34	0.26	0.27	0.62	n.a.
F	0.88	0.88	0.89	0.87	0.69	1.00	1.06	n.a.	n.a.
Sum	90.16	96.16	98.38	98.21	95.50	92.29	93.48	95.23	96.48
Less O ≡ F,Cl	0.48	0.44	0.46	0.42	0.37	0.47	0.50	0.14	0.00
Total	89.68	96.45	97.92	97.79	95.13	91.82	92.98	95.09	96.48
(Na+K)/Al	15.75	12.68	12.89	13.23	11.89	8.00	9.09	7.27	7.04
Na/(Na+K)	0.76	0.76	0.76	0.77	0.76	0.69	0.73		

1. Glass included in nepheline phenocryst.
2, 3 and 4. Glass in groundmass; each analysis is mean of 3 analyses of very uniform composition.
5, 6, 7. Glasses in single groundmass globule, with perovskite and combeite.
8, 9. Fresh, green glass in combeite and wollastonite nephelinite respectively, Oldoinyo Lengai (Peterson, 1989)

tions of the light *REE* oxides (between 12 and 15 wt.% total *REE* oxides, with Ce>La>Nd>Pr>Sm), SrO (>9 wt.%), Nb_2O_5 (>8 wt.%) and Na_2O (5 to 6 wt.%). ThO_2, FeO, BaO and K_2O are other important minor oxides, in concentrations ranging between 0.1 and 0.7 wt.%. The zones that appear brighter in BSE images (Fig. 1*h*) contain more *REE* oxides, ThO_2, SrO, BaO and Na_2O, but lower Nb_2O_5 and CaO, than the darker zones.

Overall, the phase is dominated by the perovskite, loparite, tausonite and lueshite end-member molecules, in that order (Table 12*b*); other end-member molecules and ions assigned during end-member molecule calculation comprise <10 mole %. Following the recommendations of Mitchell (1996), the BD70 mineral should be termed CeNbSr perovskite.On plots of the compositions of perovskites in both the systems perovskite-loparite-tausonite, and perovskite-loparite-lueshite (Fig. 3*a* and *b*), the perovskite forming the brighter zone (i.e. containing more *REE*) plots close to the perovskite-loparite boundary, whereas the darker zone plots further into the perovskite field. These

plots also serve to illustrate the appreciable amounts of loparite, lueshite and tausonite in solid solution. Both plots also highlight the unusual compositions of the BD70 perovskite which is unlike the perovskites from kimberlites, lamproites and peralkaline and carbonatite complexes. Significantly, they are also unlike perovskites found in ejected blocks of jacupirangite and ijolite from Oldoinyo Lengai (Dawson *et al.*, 1995*a*,*b*), that are dominated by the perovskite (*sensu stricto*) end-member molecule, with little solid solution towards loparite, tausonite and lueshite.

Magnetite
A representative analysis of the tiny opaque grains in the groundmass is SiO_2 0.05, TiO_2 9.00, Fe_2O_3 (calculated from stoichiometry) 50.7, FeO 37.7, MnO 1.37, total 98.82 wt.%. Compared with spinels in the jacupirangite and ijolite ejected blocks (Dawson *et al.*, 1995*a*,*b*), it is lower in TiO_2, and lacks the small amounts of Al_2O_3 and MgO found in the spinels in these other rocks.

TABLE 12a. Representative analyses and structural formulae of sector- zoned CeSrNb perovskite in BD70, and comparative data

	1	2	3	4		1	2
Nb_2O_5	8.36	9.00	9.74	8.80	Nb	0.824	0.864
SiO_2	0.00	0.02	<0.01	0.38	Si	0.000	0.008
ThO_2	0.45	0.30	0.76	n.a	Th	0.024	0.016
TiO_2	43.6	44.8	39.65	39.98	Ti	7.147	7.140
La_2O_3	7.01	5.12	30.80*	9.16	La	0.564	0.401
Ce_2O_3	7.79	6.19	0.00	14.04	Ce	0.622	0.481
Pr_2O_3	0.26	0.29	n.a	n.a	Nd	0.082	0.069
Nd_2O_3	1.05	0.92	n.a	n.a	Sm	0.011	0.005
Sm_2O_3	0.15	0.07	n.a	n.a	Pr	0.021	0.022
FeO	0.67	0.66	0.36	0.77	Fe	0.122	0.116
CaO	13.3	16.7	5.00	2.74	Ca	3.093	3.786
SrO	9.53	9.24	3.42	8.02	Sr	1.206	1.137
BaO	0.57	0.26	0.00	0.35	Ba	0.049	0.021
Na_2O	5.69	4.92	8.32	7.76	Na	2.405	2.025
K_2O	0.17	0.13	0.13	0.15	K	0.048	0.034
Total	98.60	98.62	100.08	99.02		16.218	16.125

Structural formulae on basis of cations per 24 oxygens

1 and 2. Bright and comparatively dark zones respectively (in B.S.E. imaging), in CeSrNb perovskite in combeite nephelinite BD70.
3. Loparite, Kola peninsula (Vlasov, 1964). * = total *REE* oxides; total includes 0.75 wt.% Ta_2O_5 and 0.57% loss on ignition.
4. Strontian loparite in rheomorphic fenite, Salitre, Brazil (Haggerty and Mariano, 1983); total includes 0.34 wt.% ZrO_2, 0.10% Y_2O_3

TABLE 12b. End-member molecules in CeSrNb perovskite in BD70

Analysis in Table 12a	1	2
	Mol.%	
Perovskite $CaTiO_3$	34.53	43.57
Loparite $(Na_{0.5}Ce_{0.5})TiO_3$	32.06	26.90
Tausonite $SrTiO_3$	14.67	14.01
Lueshite $NaNbO_3$	8.01	8.79
Latrappite $Ca(Nb_{0.5}Fe_{0.5})O_3$	3.00	2.84
$BaTiO_3$	0.59	0.26
$KNbO_3$	0.59	0.42
$CaThO_3$	0.29	0.19
Cations not assigned		
Na	3.39	1.37
Ti	2.88	1.65

Discussion

Although the cores of most phenocryst phases in BD70 are compositionally similar to other phenocryst in other lavas from the volcano, and in ejected plutonic ijolite blocks, the presence of combeite and sodalite phenocrysts indicates that, even at the onset of crystallisation, the magma had exceptionally high alkali and halogen concentrations. With continuing crystallisation further peculiarities become evident as shown by higher Fe in the rims of nepheline, sodalite and pyroxene phenocrysts, higher Nb and Sr in the rims of titanite phenocrysts, and the replacement of phenocrystal apatite intially by a high-Sr variant.

The trend towards Na, K, Fe, Ti, Ba and Sr enrichment in the residual liquids, apparent in the phenocryst rims, becomes manifest even more strongly in the groundmass with the precipitation

of aegirine-rich pyroxene (enrichment in Na and Fe), Ba-lamprophyllite (Ba, Ti and Sr), CeNbSr perovskite, and the high-NaKFeS glasses, together with the high-SrBaK 'nefedovite' replacing Sr-apatite. Further, the high halogen content of the magma, intially signalled by the phenocrystal sodalite, carries through to the groundmass where sodalite continues to precipitate together with the halogen-containing phases lamprophyllite and 'delhayelite', and halogen-bearing glass.

The crystallisation of these exotic groundmass phases serves to highlight an apparent paradox. Whereas the trend towards enhancement in the alkalies, iron, incompatible elements and halogens, together with increasing oxidation state of the iron, is what might be expected during normal fractionation (and is observed in many magma series), there is no concomitant build-up of Si and Al. This is particularly highlighted in the groundmass glasses in which the Si concentra-
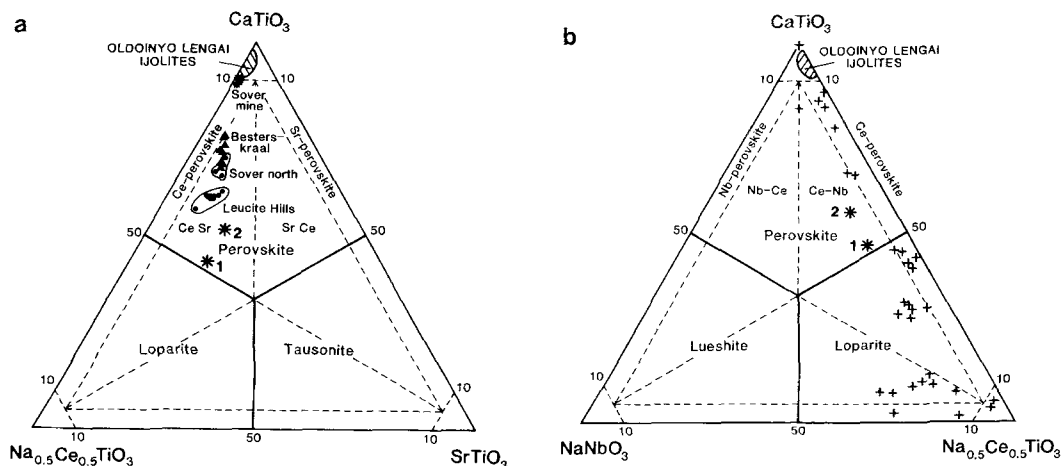
FIG. 3 (a) Compositions of Oldoinyo Lengai perovskites on perovskite-loparite-tausonite plot, adapted from Mitchell (1996). Points 1 and 2 are for BD70 (from Table 12a), other Oldoinyo Lengai data are from Dawson *et al.*, (1995a). (b) Compositions of Oldoinyo Lengai perovskites on perovskite-loparite-lueshite plot, adapted from Mitchell (1996). Oldoinyo Lengai data sources as in Fig. 3a. Crosses are perovskites and loparites from Schryburt Lake, Ontario (Platt, 1994).

tions are lower than in the whole-rock analysis, and Al is particularly low, contrasting with Na, K, Fe, and S that are in high concentrations. This is also in contrast to crystallisation trends in the plutonic blocks from the volcano in which residual glasses in the ijolites are silica-enriched (Dawson *et al.*, 1995a).

Donaldson *et al.* (1987) have pointed out the difficulties of linking the members of the silicate lava suite by fractional crystallisation of the phenocryst phases and discussion of the petrogenesis of BD70 would only be warranted within a more detailed discussion of the evolution of other nephelinites from the volcano, which is beyond the aims of this paper. However, as noted above, the unusual nature of the magma that consolidated as BD70 was apparent right from the onset of crystallisation, particularly with respect to the enhancement of alkalies relative to Al that resulted in combeite precipitation. This could not have been achieved by fractionation of nepheline or sodalite (the known high-Al phases at the volcano) from a precursor melt since, although this might produce the desired low-Al concentration seen in BD70, it would also have lead to alkali depletion and silica enhancement.

Conclusions

The crystallisation of combeite, sodalite, Balamprophyllite, 'delhayelite', KBaSr-bearing phosphate, CeSrNb perovskite and NaFe-rich glass in the groundmass of this combeite-bearing lava, together with the presence of combeite and sodalite phenocrysts, point to an exceptional concentration of alkalies, Ba, Sr and halogens. The observed alkali concentrations relative to alumina could not have been achieved by modification of a precursor nephelinite by nepheline and/or sodalite fractionation since this would have lead to alkali depletion and silica enhancement. Clearly, some other process must have been responsible for the genesis of this most unusual rock.

Acknowledgements

References

Chao, G.Y. (1971) Carletonite $KNa_4Ca_4Si_8O_{18}(CO_3)_4$ $(F,OH).H_2O$, a new mineral from Mount St.Hilaire, Quebec. *Amer. Mineral.,* **56**, 1855–66.

Dawson, J.B. (1962) The geology of Oldoinyo Lengai. *Bull. Volcanol.,* **24**, 349–87.

Dawson, J.B., Smith, J.V. and Steele, I.M. (1989) Combeite $(Na_{2.33}Ca_{1.74}others_{0.12})Si_3O_9$ from Oldoinyo Lengai, Tanzania. *J. Geol.,* **97**, 365–72.

Dawson, J.B., Smith, J.V. and Steele, I.M. (1995*a*) Petrology and mineral chemistry of plutonic igneous xenoliths from the carbonatite volcano, Oldoinyo Lengai, Tanzania. *J. Petrol.,* **36**, 797–26.

Dawson, J.B., Pinkerton, H., Norton, G.E., Pyle, D.M., Browning, P., Jackson, D. and Fallick, A.E. (1995*b*) Petrology and geochemistry of the Oldoinyo Lengai lavas extruded in November, 1988; magma source, ascent and crystallisation. In: *Carbonatite Volcanism* (K. Bell and J. Keller, eds). IAVCEI Proceedings in Volcanology, **4**, Springer, Berlin, 47–69.

Deer, W.A., Howie, R.A. and Zussman, J. (1971) *Rock-forming Minerals.* Vol. **4**, *Framework Silicates.* London, Longmans.

Donaldson, C.H., Dawson, J.B., Kanaris-Sotiriou, R., Batchelor, R.A. and Walsh, J.N. (1987) The silicate lavas of Oldoinyo Lengai, Tanzania. *Neues Jahrb. Mineral. Abh.,* **156**, 247–79.

Fersman, A.E. and Bonshtedt, E.M. (1937) *Minerals of the Khibina and Lovozero Tundras.* Lomonossov Inst. Acad Sci. U.S.S.R. (In Russian).

Gard, J.A. and Taylor, H.F.W. (1957) An investigation of two new minerals: rhodesite and mountainite. *Mineral. Mag.,* **31**, 611–23.

Haggerty, S.E. and Mariano, A.N. (1983) Strontian loparite and strontio-chevkinite: Two new minerals in rheomorphic fenites in the Parana Basin carbonatites, Brazil. *Contrib. Mineral. Petrol.* **84**, 365–81.

Hogarth, D.D. (1989) Pyrochlore, apatite and amphibole: distinctive minerals in carbonatite. In: *Carbonatites: Genesis, and Evolution* (K. Bell, ed.). London, Unwin Hyman, 106–48.

Johnsen, O., Nielsen, T.F.D. and Rønsbo, J. G. (1994) Lamprophyllite and barytolamprophyllite from the Tertiary Gardiner Complex, East Greenland. *Neues Jahrb. Mineral. Mh.,* 328–36.

Khomyakov, A.P. (1995) *Mineralogy of the Hyperagpaitic Rocks,* Oxford, Clarendon Press.

Mitchell, R.H. (1996) Perovskites: a revised classification scheme for an important rare earth element host in alkaline rocks. In: *Rare Earth Minerals: Chemistry, Origin and Ore Deposits* (A.P. Jones, F. Wall and C.T. Williams, eds), Chapman and Hall, London. 41–76.

Pecora, W.T. (1942) Nepheline syenite pegmatites, Rocky Boy Stock, Bearpaw Mountains, Montana. *Amer. Mineral.,* **27**, 397–424.

Peterson, T.D. (1989) Peralkaline nephelinites: I. Comparative petrology of Shombole and Oldoinyo L'engai, East Africa. *Contrib. Mineral. Petrol.,* **101**, 458–78.

Platt, R.G. (1994) Perovskite, loparite and Ba-Fe hollandite from the Schryburt Lake carbonatite complex, northwestern Ontario, Canada. *Mineral. Mag.,* **58**, 49–57.

Pochou, J.-L. and Pichoir, F. (1991) Quantitative analysis of homogeneous or stratified microvolumes applying the model "PAP". In: *Electron Probe Quantitation* (K.F.J. Heinrich and D.E. Newbury, eds). Plenum Press, New York, 31–75.

Sahama, Th.G. and Hytönen, K. (1957) Götzenite and combeite, two new silicates from the Belgian Congo. *Mineral. Mag.,* **31**, 503–10.

Sahama, Th.G. and Hytönen, K. (1959) Delhayelite, a new silicate from the Belgian Congo. *Mineral. Mag.,* **32**, 6–9.

Stoppa, F., Sharygin, V.V. and Cundari, A. (1997) New mineral data from the kamafugite-carbonatite association: The melilitolite from Pian di Celle, Italy. *Mineralogy and Petrology,* **61** (in press).

Vlasov, K.A. (1964) *Geochemistry,mineralogy and economic deposits of the rare elements:* Vol. **2**, *Mineralogy of the rare elements, Nauka, Moscow* (In Russian).